



## NRC Publications Archive Archives des publications du CNRC

### **Risk of condensation and mold growth in highly insulated wood-frame walls**

Saber, Hamed H.; Lacasse, Michael A.; Ganapathy, G.; Plescia, Silvio;  
Parekh, Anil

This publication could be one of several versions: author's original, accepted manuscript or the publisher's version. /  
La version de cette publication peut être l'une des suivantes : la version prépublication de l'auteur, la version acceptée du manuscrit ou la version de l'éditeur.

#### **Publisher's version / Version de l'éditeur:**

*Buildings XIII: Thermal Performance of Exterior Envelopes of Whole Buildings, 2016-12*

#### **NRC Publications Record / Notice d'Archives des publications de CNRC:**

<https://nrc-publications.canada.ca/eng/view/object/?id=f49d9079-06c7-4d25-ab08-544058b85c73>  
<https://publications-cnrc.canada.ca/fra/voir/objet/?id=f49d9079-06c7-4d25-ab08-544058b85c73>

Access and use of this website and the material on it are subject to the Terms and Conditions set forth at

<https://nrc-publications.canada.ca/eng/copyright>

READ THESE TERMS AND CONDITIONS CAREFULLY BEFORE USING THIS WEBSITE.

L'accès à ce site Web et l'utilisation de son contenu sont assujettis aux conditions présentées dans le site

<https://publications-cnrc.canada.ca/fra/droits>

LISEZ CES CONDITIONS ATTENTIVEMENT AVANT D'UTILISER CE SITE WEB.

**Questions?** Contact the NRC Publications Archive team at

PublicationsArchive-ArchivesPublications@nrc-cnrc.gc.ca. If you wish to email the authors directly, please see the first page of the publication for their contact information.

**Vous avez des questions?** Nous pouvons vous aider. Pour communiquer directement avec un auteur, consultez la première page de la revue dans laquelle son article a été publié afin de trouver ses coordonnées. Si vous n'arrivez pas à les repérer, communiquez avec nous à PublicationsArchive-ArchivesPublications@nrc-cnrc.gc.ca.



# Risk of Condensation and Mold Growth in Highly Insulated Wood-Frame Walls

**Hamed H. Saber, PhD**

**Michael A. Lacasse, PhD, PEng**

**G. Ganapathy, BEng (ME)**

**Silvio Plescia, PEng**

**Anil Parekh, MASc**

## ABSTRACT

*A research study was conducted to investigate the risk of condensation and mold growth in 2x6 wood-framing wall assemblies associated with increasing the thermal resistance (R-value) of cavity insulation for various scenarios of exterior insulation products. Based on the current construction practices, a set of three wall assemblies with different types of exterior insulation systems were chosen for field study with different R-values. In the first phase of this study, the hygrothermal model was benchmarked against the test data of full scale wood-framing wall systems. The predications of the model were in good agreement with the test data. Thereafter, the model was used to conduct parametric study to assess the risk of condensation of these wall assemblies when they were subjected to different air leakage rates for various climate zones. Both the numerical results and the field monitoring data showed different behaviours of exterior insulation strategies. The results of the hygrothermal performance were expressed using the mold index criteria, which allowed sufficient resolution to assess the risk of moisture condensation and related risk of mold growth in the wall assemblies. The results showed as well that adding exterior insulation of different water vapor permeance has resulted in lower risk of condensation and mold growth than the reference wall system (i.e. without exterior insulation).*

## INTRODUCTION - PROJECT OVERVIEW

Given the heightened interest of homebuilders to provide homes that met or exceeded Energy Star requirements, and their voiced concerns regarding “super-insulated” homes, the intent of this work was to demonstrate compliance of a set of highly-insulated wall assemblies as compared to a code compliant reference wall in respect to their anticipated thermal and hygrothermal performance when subjected to Canadian climate extremes. On the basis of providing useful information to building practitioners, the National Research Council of Canada (NRC) undertook field monitoring and numerical modelling to investigate the risk of condensation in wall assemblies having different combinations of increased thermal resistance (R-value) of insulation for selected insulation products.

The field monitoring of different wall assemblies was undertaken in the NRC’s Field Exposure of Walls Facility (FEWF) in a two-phase, two year project. Three wall assemblies were tested in the initial year of Phase 1 of the project and another three wall assemblies were tested in Phase 2 of the second project year. A detailed description of the wall assemblies of Phase 2 are available in [1]; this paper focuses on describing the results derived from the initial three wall assemblies evaluated in Phase 1.

In Phase 1, three 1219 mm x 1829 mm (4 ft. x 6 ft.) test specimens having conventional 38 mm x 140 mm (2 x 6-in.) wood-frame walls were constructed using different types of exterior insulation products that included: 25 mm (1-in.) EPS; 51 mm (2-in.) XPS, and; 76 mm (3-in.) Mineral Fibre (MF) insulation. The three specimens were installed side-by-side in the FEWF and exposed to local climate conditions of Ottawa over a one year period; the test period started in August, 2013 and ended in October, 2014.

**H.H. Saber:** Associate Research Officer, NRC-Construction, National Research Council Canada; **M.A. Lacasse:** Senior Research Officer, NRC-Construction, National Research Council Canada; **G. Ganapathy:** Technical Officer, NRC-Construction, National Research Council Canada; **S. Plescia:** Senior Researcher, Policy and Research Division, Canada Mortgage and Housing Corporation; **A. Parekh:** Senior Researcher, Buildings and Renewables Group, Natural Resources Canada

On the basis of results obtained from monitoring the response of the respective wall assemblies to local climate conditions, the numerical hygrothermal model hygIRC-C was benchmarked against selected experimental data. Thereafter, the model was used to conduct a parametric analysis to investigate the risk of condensation and mold growth in the respective wall assemblies subjected to different climatic conditions for a select set of locations in Canada. A description of the hygIRC numerical hygrothermal simulation model and record of benchmarking exercises are available in [2].

In this paper, results are provided for benchmarking the hygIRC-C numerical simulation model against experimental test data. Thereafter, information derived from simulations is provided on the risk of formation of condensation and subsequent mold growth within the three configurations of wood-frame wall assembly as were tested in the FEWF. The simulations considered subjecting each of the three walls to the climatic conditions of five locations in Canada and for which the climate varied as being mild-wet to cold-wet, and cold-wet to cold-dry.

## DESCRIPTION OF WALL SPECIMENS

The three wall test specimens of Phase 1 (1219 mm x 1829 mm / 4 ft. x 6-ft.) consisted of 38 mm x 140 mm (2 x 6-in.) wood-frame walls installed side-by-side in the FEWF (Figure 1). The different material layers and the dimensions of the wall specimens are given in Figure 2 to Figure 4. The backup wall for all three design strategies consisted of interior drywall (12.7 mm / 0.5 in. thick), polyethylene air and vapour barrier (6 mil thick), 38 mm x 140 mm (2 x 6-in.) wood-frame wall with friction-fit glass fibre batt insulation of R-24, and Oriented Strand Board (OSB) (11 mm / 7/16 in. thick). The test specimens were constructed by adding different types of exterior insulation products of different thicknesses to the backup wall. The first wall (Wall 1; Figure 2,) was constructed by adding an expanded polystyrene (EPS) layer of 25 mm (1 in) thick onto the OSB sheathing. The second wall (Wall 2; Figure 3) was constructed with a 51 mm (2 in) thick extruded polystyrene (XPS) panel. The final wall (Wall 3; Figure 4) was constructed with 76 mm (3 in) thick mineral fibre insulation.

As a part of the test protocol, more fully described in [1], all Heat Flux Transducers (HFTs) used in the three test specimens were calibrated according to ASTM C-1130 “Standard Practice for Calibrating Thin Heat Flux Transducers” [3]. The locations of the HFTs in the respective test specimens are shown in Figure 2 to Figure 4. The uncertainty of the heat flux measurements was  $\pm 5\%$ .

## MODEL BENCHMARKING

Having previously benchmarked the present model to several tests undertaken in controlled laboratory conditions as described in [2, 4], a subsequent and important step was to benchmark the present model against the field measurements for the three wall systems previously described. Information is provided regarding assumptions in completing the transient numerical simulations and initial and boundary conditions that were used in conducting model benchmarking.

### Transient Numerical Simulations

This section presents the assumptions and initial and boundary conditions that were used in conducting the numerical simulations for respective wall test specimens. The hygrothermal properties of insulation and other wall components were either measured or taken from the in-house database of hygrothermal material properties [5].

**Assumptions.** It was assumed that all material layers were in direct contact with one another (i.e. the interfacial thermal resistances between all material layers were neglected). The emissivity of all surfaces that bounded the airspaces (i.e. airspaces between exterior insulations, furring strips and vinyl siding) was taken equal to 0.9 [6]. The effects of heat transfer by conduction, convection and radiation within these airspaces on the thermal performance of wall assemblies were also determined.

**Initial and boundary conditions.** The initial temperature in all material layers of the respective wall specimens (Wall 1, 2 and 3) was assumed uniform and equal to 10.0 °C. Since this initial temperature was not the same as that of

the test, it was anticipated that the predicted dynamic response of the different wall specimens in the initial test period (e.g. the first 24 – 48 hr) would be different from that obtained in the test itself. The boundary conditions on the top and bottom surfaces of the wall systems were assumed to be adiabatic (i.e. no edge heat losses). The outdoor surface of the vinyl siding and the indoor surface of the gypsum board were respectively subjected to a temperature boundary condition for all wall systems. The temperatures on the outdoor and indoor surfaces of the respective wall specimens, and that changed over time, were taken equal to that measured on these surfaces.

### Comparison between Model Predictions and Measurements

To benchmark the hygroIRC-C model, transient numerical simulations were conducted for the three wall test specimens (Figure 1). A full description of all instrumentation (i.e. thermocouples, Heat Flux Transducers (HFTs), Pressure (P) sensors, and Relative Humidity (RH) sensors) and experimental data are available in [1]. In each wall system, three HFTs were used to measure the heat flux at the middle (mid-height and mid-width, as given in Figure 2, Figure 3 and Figure 4) of each of the respective wall test specimens at three interfaces; namely:

- (i.) HFT1 at the interface between the airspace and exterior insulation;
- (ii.) HFT2 at the interface between the exterior insulation and OSB panel, and;
- (iii.) HFT3 at the interface between the polyethylene air barrier membrane and gypsum panel.

For the EPS wall specimen (Wall 1), Figure 5-i, Figure 5-ii and Figure 5-iii show comparisons between the measured and predicted values of heat flux during the test period. In these figures, time = 0 at which experimental data was collected corresponded to August 11, 2013 at 12:37 AM. Unlike the other wall specimens, the HFT1 located at the interface between the airspace and exterior insulation in Wall 1 was not functioning properly during the entire test period (Figure 5-i). However, as shown in Figure 5-ii, the predicted heat flux at the EPS – OSB interface is in good agreement with the measurements from HFT2. Similarly, Figure 5-iii shows that the predicted heat flux at the poly – gypsum interface is in good agreement with measurements from HFT3.

Figure 6-i, Figure 6-ii and Figure 6-iii show comparisons between the measured and predicted values of heat flux during the test period at different locations for the XPS wall specimen (Wall 2). As shown in these figures, the predicted values of heat flux were in good agreement with the measured values at each of the respective interfaces, specifically at the: airspace – XPS interface (Figure 6-i), XPS – OSB interface (Figure 6-ii), and the poly–gypsum interface (Figure 6-iii).

Finally, for the wall specimen having mineral fibre insulation (Wall 3), comparisons are provided in Figure 7-i, Figure 7-ii and Figure 7-iii and in which are shown the predicted values of heat flux that were in good agreement with the measured values at each of the respective interfaces, specifically at the: airspace–mineral fibre interface (Figure 7-i), the mineral fibre–OSB interface (Figure 7-ii), and the poly–gypsum interface (Figure 7-iii).

In summary, the results presented in this section show that the predicted values of heat flux at different locations in the wall assembly are in good agreement with the measured values of heat flux for the three walls, namely the: EPS wall specimen (Figure 5), XPS wall specimen (Figure 6), and mineral fibre wall specimen (Figure 7).

It is not possible to complete the benchmarking of the model in respect to moisture transport on the basis of the field trials undertaken in the FEWF. This requires conducting experiments in a controlled environment after first conditioning the test specimens to known levels of moisture content. In fact the model has previously been benchmarked in controlled conditions as is described in more detail in [2, 4].

Thus, after benchmarking the present model in respect to heat flux, and having previously benchmarked the model to several tests undertaken in field and controlled laboratory conditions as indicated in [2, 4], this model was used with confidence to investigate the risk of condensation and mold growth in different wall assemblies with exterior insulations when these walls were subjected different Canadian climatic conditions.

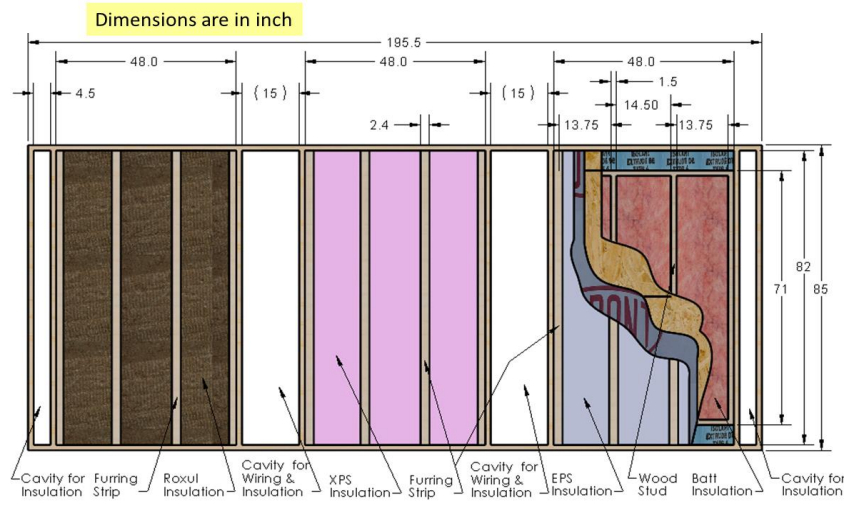
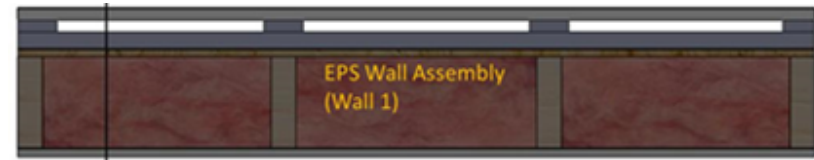


**Figure 1.** Schematic of three residential 38 mm x 140 mm (2 x 6 in.) wood-frame wall test specimens installed side-by-side in the FEWF



- Vinyl siding
- 1.5-in. x 7/16" thick vertical furring strips
- **25 mm (1-in.) EPS rigid foam insulation (exterior insulation)**
- Sheathing membrane
- 11 mm OSB wood-sheathing
- 2x6-in. nominal stud cavity with R24 glass fiber insulation batts
- 6 mil poly air/vapour barrier
- ½ in. painted drywall



**Figure 2.** Horizontal cross-section through EPS wall assembly showing locations of Heat Flux Transducers, HFTs (Wall 1)



- Vinyl siding
- 1.5 in wide x 7/16" thick vertical furring strips
- **51 mm (2 in.) XPS rigid foam insulation (exterior insulation)**
- Sheathing membrane
- 11 mm OSB wood-sheathing
- 2x6-in. nominal stud cavity with R24 glass fiber insulation batts
- 6 mil poly air/vapour barrier
- ½ inch painted drywall



**Figure 3.** Horizontal cross-section through XPS wall assembly showing locations of Heat Flux Transducers, HFTs (Wall 2)



- Vinyl siding
- 1.5-in. x 7/16" thick vertical furring strips
- **76 mm (3-in.) semi-rigid mineral fibre insulation (exterior insulation)**
- Sheathing membrane
- 11 mm OSB wood-sheathing
- 2x6-in. nominal stud cavity with R24 glass fiber insulation batts
- 6 mil poly air/vapour barrier
- ½ in. painted drywall



**Figure 4.** Horizontal cross-section through mineral fibre wall assembly showing locations of Heat Flux Transducers, HFTs (Wall 3)

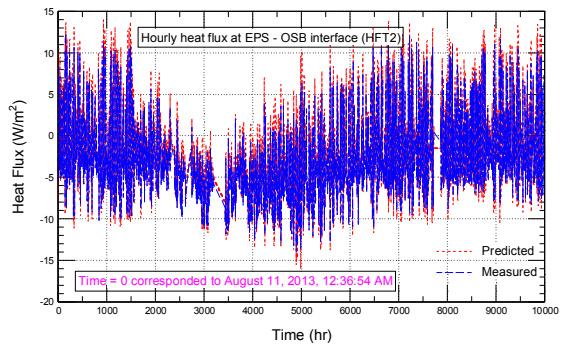
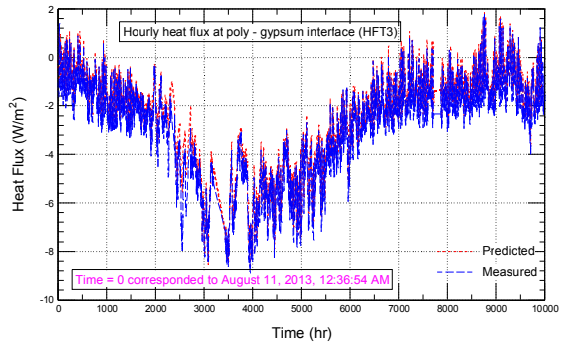
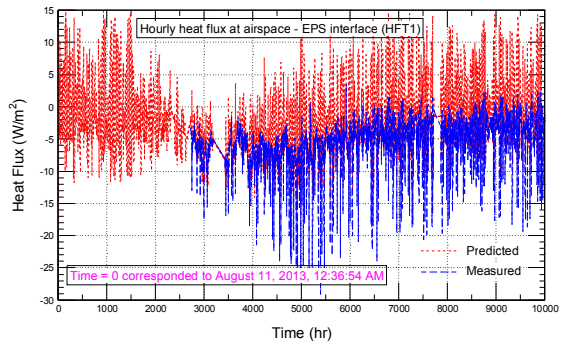


**Figure 5.** Wall 1 (EPS) — Comparison between predicted & measured heat fluxes at interface: (i) airspace–EPS; (ii) EPS–OSB; (iii) poly–gypsum

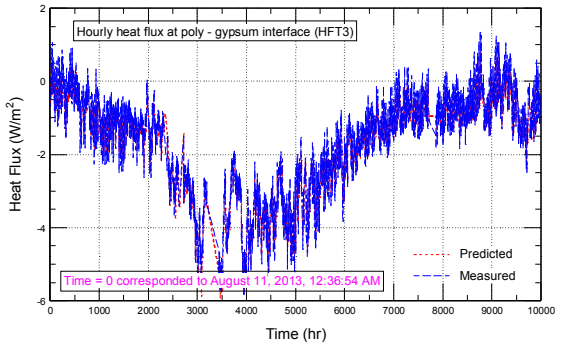
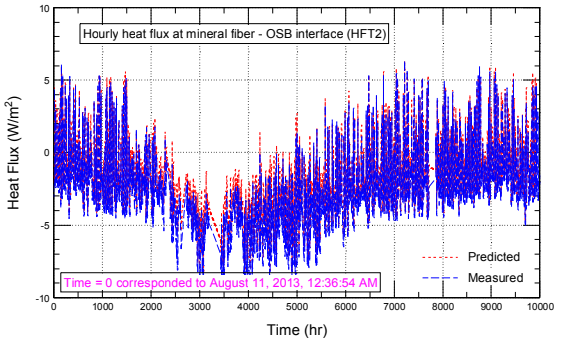
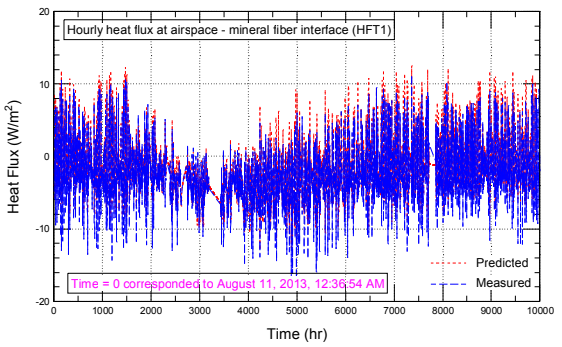


**Figure 6.** Wall 2 (XPS) — Comparison between predicted & measured heat fluxes of interface: (i) airspace–XPS; (ii) XPS–OSB; (iii) poly–gypsum

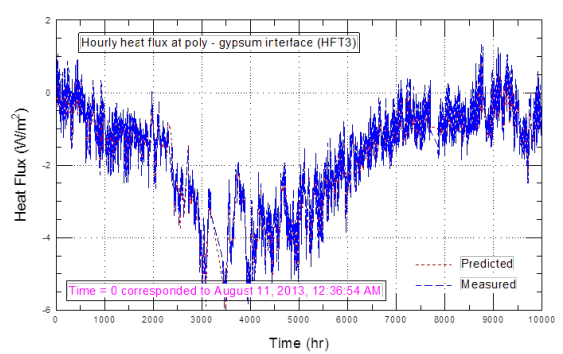
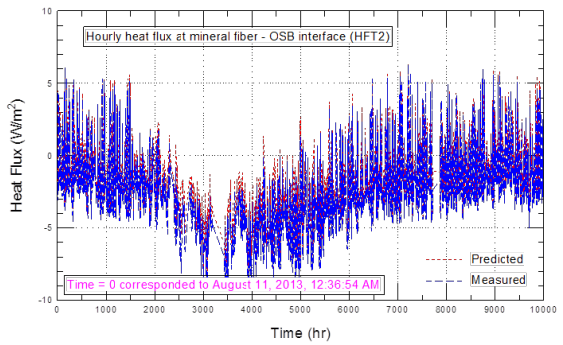
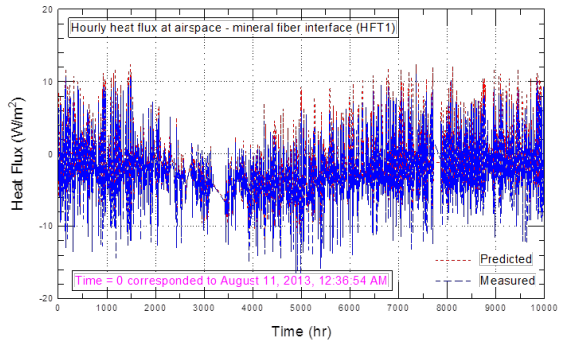


**Figure 7.** Wall 3 (Mineral fibre) — Comparison between predicted & measured heat fluxes of interface: (i) airspace–mineral fibre; (ii) mineral fibre–OSB; (iii) poly–gypsum

## SIMULATION OF WALL ASSEMBLIES

### Wall Assembly Configurations for Simulation and Simulation Parameters

Hygrothermal simulations of all wall assemblies were conducted using the hygIRC-C model and using the construction details common to all wall assemblies to be modelled as listed in Table 1. For each of the materials or components specified, the rationale for the selection of specific materials is also given in this table.

**Table 1. Construction details common to all wall assemblies to be modelled**

Material selection	Rationale
Exterior finish consisting of vinyl cladding installed on 19 mm strapping	To minimize impact of water ingress from the exterior
Weather-resistive barrier (WRB) with WVP of 1400 ng/(Pa•s•m <sup>2</sup> ) (25 US perm) such as spun bonded polyolefin membrane	Common construction and highly permeable so as not to limit application of insulation materials for which selection of a more vapour tight material might otherwise affect intent of project
Wood-frame construction (2 x 6 in.); framing at 16-in. on center	Currently, most common construction framing used in housing
Vapour barrier with WVP of 60 ng/(Pa•s•m <sup>2</sup> )	NBCC 2010 minimum requirement 9.25.4.2. (see [7])
Interior finish of 12.5 mm gypsum board	Currently most common construction method for interior finish

Figure 8 shows a schematic of the code-compliant reference wall assembly to which the performance of test specimens Wall 1, 2 and 3 was compared. Whereas the simulated results for moisture content and temperature are produced for every location within the wall system and at every 1 hour, an analysis of results was performed to establish those locations in the wall that had the greatest susceptibility to risk of condensation; this permitted rationalizing the presentation of results. Post-processing of simulation results and reporting thus focused on the locations shown in Figure 8.

### Simulation Conditions for Parametric Study

In this section, the different simulation conditions are discussed and that were used to conduct the numerical simulations for all wall assemblies shown in Figure 2 to Figure 4 and Figure 8 (see Table 2).

**Vapour Barrier Conditions.** As provided in Subsection 9.25.4 of the NBCC [7], the current maximum allowable WVP value for vapour barriers is 60 ng/(Pa•s•m<sup>2</sup>). The parametric study was conducted using a vapour barrier with a WVP of 60 ng/(Pa•s•m<sup>2</sup>) as provided in Table 1.

**Air Leakage Conditions.** All cases were modeled with some air flow introduced through openings into the assembly, as this is a likely scenario given the imperfections of the air barrier system of wall assemblies. Additionally, completing the investigation without considering the effects of air leakage would not create useful results in terms of assessing the risk to the formation of condensation in wall assemblies given that exfiltration of indoor air to the wall assembly is the primary cause for the formation of condensation in the assembly itself.

It was assumed that the path for air movement (shown in Figure 8) was initiated at the interior of the assembly at the bottom of the wall and thereafter moisture was deposited along the interior face of the sheathing panel and exited through the top of the wall. This air leakage path was one of the scenarios used in the study by Ojanen and Kumaran [8] in which it was assumed that air would move through imperfections that existed at the wall top plate and specifically at the interface between the interior face of the exterior sheathing and the exterior of the top plate. For the code-compliant reference wall (i.e. no exterior insulation), this air leakage path is shown Figure 8, a similar path was assumed for Walls 1, 2 and 3.

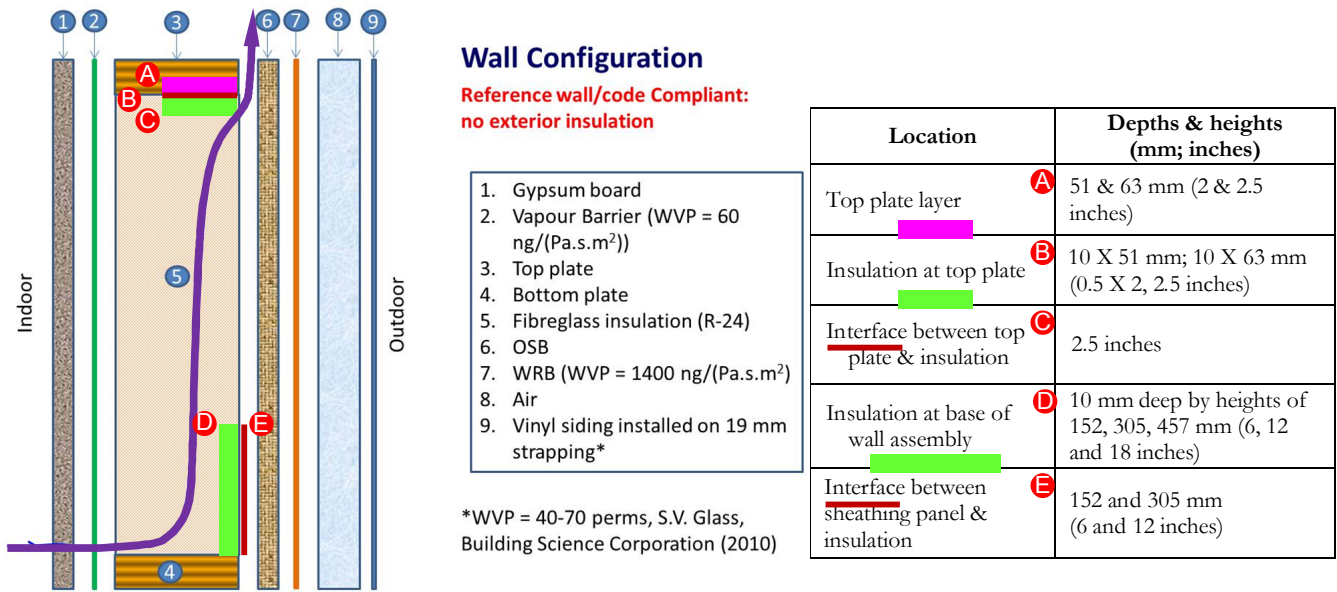


**Figure 8.** Schematic of reference wall assembly/code compliant configuration showing different component layers and assumed path of air flow through assembly (no exterior insulation)

The air leakage rate for all cases in all locations was set to 0.1 L/(s•m<sup>2</sup>) at 75 Pa, which was an assumption used in at least one previous study (see [4, 8, 9]). These air leakage conditions are those assumed for the wall components of a home and would be roughly an order of magnitude smaller than the whole house air leakage of an R-2000 or ENERGY STAR qualified home, as provided by Natural Resources Canada (NRCAN).

The impact of this assumption on the hygrothermal performance was investigated in a sensitivity analysis, by modelling a wall assembly with different air leakage rates ranging between 0 and 0.1 L/(s•m<sup>2</sup>) at 75 Pa. The results from such an analysis permitted deriving the least performing and most vulnerable wall assembly with respect to the formation of condensation and the risk to the formation of mold within the assembly. In this paper, rates of air leakage referred to as 0%, 50% and 100% of air leakage relate, respectively, corresponded to 0.0, 0.05 and 0.1 L/(s•m<sup>2</sup>) at 75 Pa. As indicated later, the results of the sensitivity study supported the selection of 0.1 L/(s•m<sup>2</sup>) at 75 Pa as a means of challenging the wall system with moisture ingress from air leakage.

**Approach to Simulation of Air Leakage.** In the present study, the air leakage rate ( $Q$ ) as a function of the total pressure differential across the wall assemblies ( $\Delta P_{tot}$ ) is given as:

$$Q = a \Delta P_{tot}^n \quad ((1))$$

In a previous NRC project “Wall Energy Rating, WER” [10-13], the air leakage rates were measured for a number of 2 x 6-in. wood-frame walls having different types of thermal insulation in the wall cavities including open cell spray foam, closed cell spray foam, and glass fibre. For the full-scale wall systems with and without penetrations and having glass fibre insulation, the average value of the exponent ‘n’ in Eq. ((1) was 0.7; this value was used in this study. The value of coefficient ‘a’ in Eq. ((1) was determined to satisfy the condition at which the air leakage rate is 0.1 L/(s•m<sup>2</sup>) at  $\Delta P_{tot} = 75$  Pa when the exponent n = 0.7. As such, the value of coefficient ‘a’ is equal 0.00487 L/(s•m<sup>2</sup>•Pa<sup>0.7</sup>) where Q in is L/(s•m<sup>2</sup>) and  $\Delta P_{tot}$  in Pa.

In Eq. ((1), the total pressure across the building envelope can be calculated as:

$$\Delta P_{tot} = \Delta P_{wind} + \Delta P_{st} + \Delta P_{ven} \quad ((2)$$

Where:

$\Delta P_{wind}$ : pressure differential due to wind;

$\Delta P_{st}$ : pressure differential due to the stack effect; and

$\Delta P_{ven}$ : the pressure differential due to mechanical ventilation system (i.e. pressurization or depressurization due to heating and cooling conditions);  $\Delta P_{ven}$  was neglected and thus  $\Delta P_{ven} = 0$ .

The full details for calculating both the pressure differential due to the stack effect and wind pressure differential given different climatic conditions are available in reference [4]. As indicated in [4], the greater the exfiltration rate the higher the risk of formation of condensation and mold growth within the wall assembly; the wall is located at the third storey and facing the direction of the highest exfiltration rate. This would thus represent the worst case scenario for the risk of formation of condensation and mold growth within the wall cavity. As such, all wall assemblies that were investigated in this study represent wall assemblies of the third storey of low-rise buildings.

### Exterior Climatic Conditions

**Locations.** All wall assemblies were subjected to different climatic conditions of five different locations within Canada and having differing values of Heating Degree Days (HDD) and Moisture Index (MI), namely:

- Vancouver, BC (mild, wet, HDD18 = from 2600 to 3100, MI = 1.44),
- St. John's, NL (cold, wet, HDD18 = 4800, MI = 1.41),
- Ottawa, ON (cold, dry, HDD18 = 4440 - 4500, MI = 0.84),
- Edmonton, AB (cold, dry, HDD18 = 5120, MI = 0.48), and
- Yellowknife, NT (cold, dry, HDD18 = 8170, MI = 0.58).

**Orientation of wall assemblies.** The wall assemblies of the third storey of low-rise buildings were modeled in the orientation showing the highest average annual air exfiltration rate. The walls were assumed to be shaded to minimize the impact of solar-driven moisture ingress into the assembly and likewise to minimize the solar drying effect on the wall. However, diffuse radiation was taken into consideration.

**Weather Data.** Hygrothermal simulations were conducted for a period of two years. The first year corresponded to an average year (conditioning year, where equal drying and wetting potential exists) and the second year corresponded to a wet year. Note that the wet year in each location was the worst-case situation given that the drying potential for a wall assembly is limited during a wet as compared to a drier year. The weather data of the different locations were obtained from the NRC's weather database.

### Indoor Conditions

Regarding to the indoor moisture load, the water vapour pressure differential across the wall assembly (from indoor to outdoor) corresponded to a moisture load of 5.2 g/m<sup>3</sup>. This indoor moisture load is consistent with that used in previous studies, in which a moisture load of 7.1 L/day was chosen for a 1 storey, 80 m<sup>2</sup> house, with indoor temperature of 21°C, water vapour pressure differential close to 700 Pa ( $\Delta P_v = P_{v, indoor} - P_{v, outdoor} = 700$  Pa), and 0.3 ACH by mechanical ventilation; this is referred to as Option-A in which the indoor relative humidity (RH<sub>ind</sub>) for the climatic conditions of Ottawa, as an example, are provided. As shown in this figure, Option-A resulted in a high value for RH<sub>ind</sub>, that at times exceeded 100%.

Three additional options for the indoor RH profile were also considered within a period of one year as shown in Figure 9; these were:

- Option-A  $\Delta P_v = 700 \text{ Pa}$
- Option-B This option was based on the method given in ASHRAE 160.
- Option-C Similar to Option-A (i.e.  $\Delta P_v = 700 \text{ Pa}$ ) but the value of  $RH_{ind}$  was capped at 70%.
- Option-D Based on ASHRAE 160; interior RH during winter reduced with cold temp.

Option-C was the recommended option to evaluate the indoor relative humidity [2, 4] and was used in this study to conduct all numerical simulations of different wall assemblies that are listed in Table 2. Other indoor conditions (i.e. indoor temperature) were set according to that provided in the ASHRAE Standard 160 [14] with respect to recommendations for conditioned space.

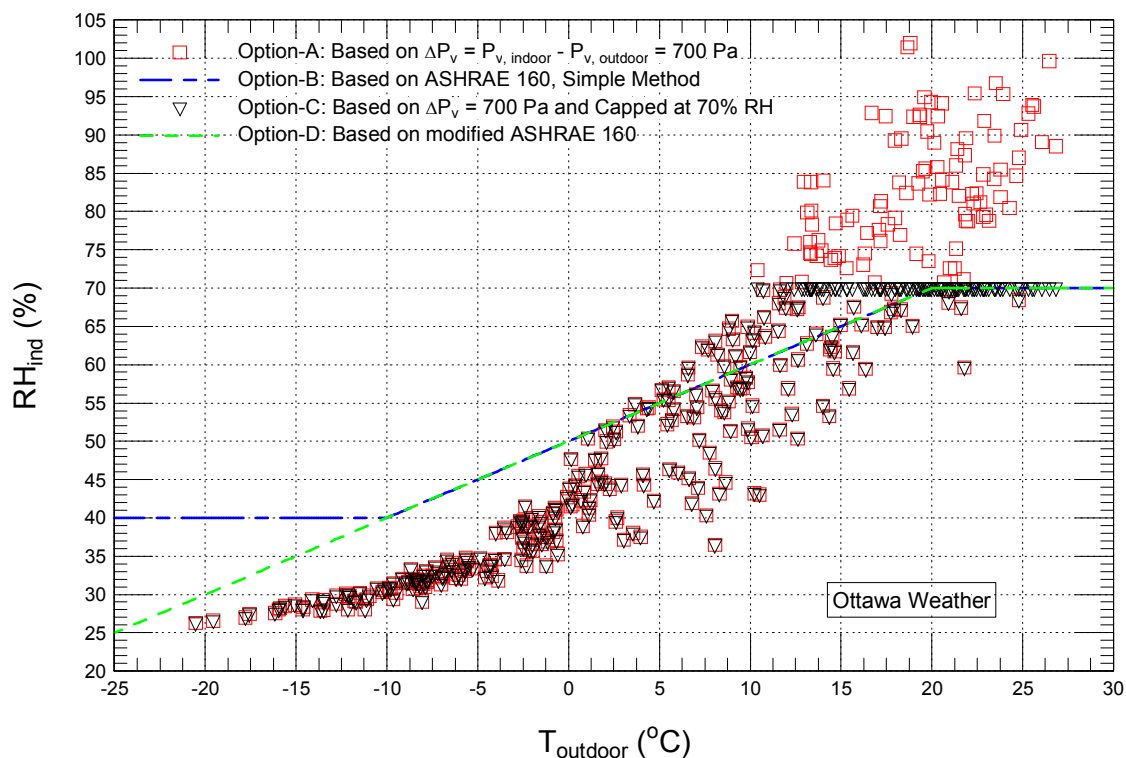


Figure 9. Different options for indoor relative humidity (Ottawa weather)

### Initial Conditions

The initial temperature in all layers of the wall assemblies were taken equal to 21°C and the initial moisture content of all material layers corresponded to a relative humidity of 50%.

### Material Properties

The hygrothermal properties for the exterior insulations in Wall 1 (EPS), Wall 2 (XPS) and Wall 3 (mineral fibre) were measured in NRC's laboratory. The different types of exterior insulation products used in this study are listed in Table 2. All wall assemblies incorporated a sheathing panel made of 11 mm (7/16 in) thick OSB; of importance was the choice of WVP for the panel. Glass [15] has compiled the available data for the WVP of OSB (11 mm thick). The recommended values by Glass [15] for the WVP of OSB as a function of RH were used in the numerical simulations. The hygrothermal properties of the other material layers shown in Figure 8 were obtained from NRC's material database [5].

**Table 2. Wood framed (2 x 6-in.) wall systems with exterior insulations\***

Parameter	Wall 1	Wall 2	Wall 3
	Exterior Insulation Type		
	EPS	XPS	Mineral fibre
Thickness (in)	1 (25 mm)	2 (51 mm)	3 (76 mm)
Dry Density (kg/m <sup>3</sup> )	18	26	122
Dry Thermal Conductivity (W/(m•K))	0.0369	0.0290	0.0347
Vapor Permeability (kg•m/(s•m <sup>2</sup> •Pa))	2.91E-12	1.39E-12	1.62E-10
Total Vapor Permeance (ng/(s•m <sup>2</sup> •Pa))	114.4	27.4	2129
Vapor Permeance ((ng/(s•m <sup>2</sup> •Pa))/25 mm)	114.4	54.9	6390
Total RSI-value (m <sup>2</sup> •K/W)	0.69	1.75	2.20
Total R-value (ft <sup>2</sup> •hr•°F/BTU)	3.91	9.95	12.47
R-value ((m <sup>2</sup> •K/W)/25.4 mm)	0.69	0.88	0.73
R-value ((ft <sup>2</sup> •hr•°F/BTU)/in)	3.9	5.0	4.2

\*2x6-in. wood-frame cavity insulation: batt insulation of R-24 (RSI-4.2)

### Summary of Simulated Conditions

A summary of the simulated conditions for all wall assemblies are provided in Table 3.

**Table 3. Summary of simulated conditions**

Criteria	Assumptions/Conditions
Pressure exponent, n	0.7 (see Eq. (1))
Predominant wall orientation	Facing the highest exfiltration rate
$\Delta P$ for stack effect	Top storey of a 3-storey building to maximize effect of exfiltration
$\Delta P$ for ventilation	Assume depressurization/pressurization from ventilation source is negligible
Air leakage rate, Q	Corresponds to 0.0, 0.05 and 0.1 L/(s•m <sup>2</sup> ) at 75 Pa
Interior moisture load	Constant water vapour pressure differential, $\Delta P_v = 700$ Pa and capped at 70% RH
Water vapour permeance of OSB	Function of RH ranging from 0-100% as recommended by Glass [15]
Modelling period	Two years – Jan to Dec: one “average” year followed by one “wet” year
Geographical locations	Ottawa (ON), Edmonton (AB), Vancouver (BC) Yellowknife (NT), and St. John’s (NL)

### ACCEPTABLE PERFORMANCE

The modelling results for each case were expressed using the mold index (M) criteria developed by Hukka and Viitanen [16], Viitanen and Ojanen [17], and Ojanen et al. [18]. The descriptions of mold index levels are provided in Table 4. The most recent mold model by Ojanen et al. [18] was used in this study to determine the mold index of different materials of the wall assemblies. In that model [18], the sensitivity of different construction materials for mold growth was classified in 4 sensitivity classes (Table 5): very sensitive, sensitive, medium resistant and resistant.

Table 6 provides the assumed correspondence of sensitivity class for materials located within the wall assembly modelled in this study. More specifically, the sensitivity class for the top and bottom plates, OSB and foam was considered “Sensitive”, whereas the sensitivity class of the materials for cavity insulation (fiber-based), drywall and membranes was considered “Medium Resistant”. The selected mold index criteria allowed sufficient resolution to assess the risk of moisture condensation.

**Table 4. Description of Mold Index (M) levels [16, 17, 18]**

M	Mold Index (M) Description of Growth Rate
0	No growth
1	Small amounts of mold on surface (microscope), initial stages of local growth
2	Several local mold growth colonies on surface (microscope)
3	Visual findings of mold on surface, < 10% coverage, or < 50% coverage of mold (microscope)
4	Visual findings of mold on surface, 10%–50% coverage, or > 50% coverage of mold (microscope)
5	Plenty of growth on surface, > 50% coverage (visual)
6	Heavy and tight growth, coverage about 100%

**Table 5. Mold growth sensitivity classes and some corresponding materials [16-18]**

Sensitivity Class	Materials	RH <sub>min</sub> (%)
Very Sensitive	Pine sapwood	80
Sensitive	Glued wooden boards, PUR with paper surface, spruce	80
Medium Resistant	Concrete, aerated and cellular concrete, glass wool, polyester wool	85
Resistant	PUR with polished surface	85

\* Minimum relative humidity needed for mold growth

**Table 6. Mold growth sensitivity classes for materials of wall assemblies**

Sensitivity Class	Material Layers of Wall Assemblies	RH <sub>min</sub> (%)*
Very Sensitive		80
Sensitive	Top plate, bottom plate, OSB, foam	80
Medium Resistant	Fiberglass insulation, gypsum, membranes	85
Resistant		85

\*Minimum relative humidity needed for mold to grow

### Approach for Assessing the Overall Performance

The overall hygrothermal performance of the different wall assemblies (i.e. Wall 1 (EPS); Wall 2 (XPS), and; Wall 3 (Mineral fibre)) evaluated in this study was assessed against the performance of the code compliant reference wall. The values of the mold index as determined from simulation results of the three walls were compared against the values of the mold index of the reference wall; adequate performance was achieved if the comparison showing value for values mold index equal to or lower than that of the reference wall.

The primary locations within the wall assemblies at risk for condensation of moisture and possible mold growth were identified as those located at either the top or bottom portion of a wall assembly. All of these “at risk” locations are shown in Figure 8. More details of these locations are available in the reference [2]. For the purpose of comparing the performance of different wall assemblies, these results are presented on basis of a simplified form using the following two parameters [2, 4]:

M<sub>AVG</sub>: Overall average value of mold index at different locations in the wall; locations are shown in Figure 8;

M<sub>MAX</sub>: Overall maximum value of mold index at different locations in the wall.

The two parameters above were determined based on a simulation period of two years, i.e., simulation of the average year followed by a wet year for the location of interest (see Figure 8). Both these values are provided for each of the different wall configurations having nominal insulation in the stud-cavity (referred to as inboard insulation) of R-24, as well as for each of the exterior insulation conditions (referred to as outboard insulation); exterior insulation conditions varied from R-0 (i.e. reference wall) to values of R-3.91, R-9.95, and R-12.47 (see Table 2). However, for the climatic conditions of Edmonton, stud-cavity insulation of R-19 was also considered in this study to allow comparison of the risk of condensation and mold growth in these walls to the case of a wall having stud-cavity insulation of R-24.

## RESULTS AND DISCUSSION

In this section, the effects of different parameters that affect the hygrothermal performance of wall assemblies are discussed. The list of wall assemblies is provided in Table 2. In this paper, in instances where the units for Water Vapour Permeance (WVP) and R-value are not reported, the units for each of these parameters are respectively,  $\text{ng}/(\text{Pa}\cdot\text{s}\cdot\text{m}^2)$  and  $\text{ft}^2\cdot\text{h}\cdot\text{F}/\text{BTU}$ . Note that all results derived for the reference wall having stud-cavity insulation of R-19 and R-24 were obtained from a previously published project report (see [4] for more details). The different parameters affecting the hygrothermal performance of walls and discussed in this section include: air leakage rate; R-value of stud-cavity insulation; and, geographical locations.

### Effect of Air Leakage Rate

The effect of the air leakage rate on the hygrothermal performance of wall assemblies listed (Table 2), as determined by the risk of mold growth in a wall assembly, permitted identifying the locations within the assembly of likely mold growth given the different air leakage rates to which it was subjected. In these analyses, the full amount of the air leakage given by Eq. (1) (i.e.  $\xi = 100\%$ ) and different percentages of that value ( $\xi = 0\%$  and  $50\%$ ) were considered.

The Mold Index (M) was calculated for different wall assemblies on the basis of the mold sensitivity classes of the different material layers within the wall assembly as provided in Table 6. It is important to point out that the locations within the wall assemblies at risk of condensation and mold growth are based on the respective air leakage paths that were considered in this study and shown in Figure 8. It is noted that a different air leakage path, however, would result in different locations within the wall assemblies at risk of condensation and mold growth.

Figure 10a and Figure 10b, respectively, show the overall average mold index ( $M_{\text{AVG}}$ ) and overall maximum mold index ( $M_{\text{MAX}}$ ) for different percentages of the air leakage rate of  $\xi = 0\%$  (no air leakage),  $50\%$ , and  $100\%$  for the wall system with exterior insulation of EPS (RSI-0.69 and WVP = 114 (R-3.9 and WVP = 2.0 US perm)), subjected to different climatic conditions. As shown in these figures, decreasing the air leakage rate resulted in decreasing the risk of condensation and mold growth, whereas no risk of condensation occurred at  $\xi = 0\%$ . For example, the values of  $M_{\text{AVG}}$  for the case of  $\xi = 50\%$  are 29%, 44%, 75%, 56% and 24% of the values of  $M_{\text{AVG}}$  for  $\xi = 100\%$ , respectively, for Ottawa, Edmonton St. John's, Vancouver, and Yellowknife (Figure 10a). Note that at a pressure difference ( $\Delta P$ ) of 75 Pa,  $\xi = 50\%$  corresponds to an air leakage of  $0.05 \text{ L}/(\text{s}\cdot\text{m}^2)$  whereas  $\xi = 100\%$  corresponds an air leakage rate of  $0.1 \text{ L}/(\text{s}\cdot\text{m}^2)$ . Furthermore, the values of  $M_{\text{MAX}}$  for the case of  $\xi = 50\%$  are 42% and 56%, 83%, 70% and 37% of the values of  $M_{\text{MAX}}$  for the case of  $\xi = 100\%$  for Ottawa, Edmonton St. John's, Vancouver, and Yellowknife, respectively (Figure 10b).

For the wall system with XPS exterior insulation of R-10 and WVP = 27, Figure 11a and Figure 11b show the effect of air leakage rate on the overall maximum and average mold index. Similar to the results obtained for the EPS wall, decreasing the air leakage rate resulted in decreasing the risk of condensation and mold growth. As shown in Figure 11a, the values of  $M_{\text{AVG}}$  for the case of  $\xi = 50\%$  are 18% and 32%, 58%, 40% and 9% of the values of  $M_{\text{AVG}}$  for  $\xi = 100\%$ , respectively for Ottawa, Edmonton St. John's, Vancouver, and Yellowknife. The corresponding values of  $M_{\text{MAX}}$  for the case of  $\xi = 50\%$  are 56% and 52%, 90%, 79%, and 26% respectively, of the values of  $M_{\text{MAX}}$  for  $\xi = 100\%$  for Ottawa, Edmonton St. John's, Vancouver, and Yellowknife (Figure 11b).

Figure 12a and Figure 12b show  $M_{AVG}$  and  $M_{MAX}$  for different air leakage rates for the wall system with mineral fibre exterior insulation of R-12.5 and WVP = 2130, when this wall was subjected to different climatic conditions. As shown in these figures, the values of  $M_{AVG}$  for  $\xi = 50\%$  are 31% and 40%, 79%, 66% and 19% of the values of  $M_{AVG}$  for  $\xi = 100\%$ , respectively, for Ottawa, Edmonton St. John's, Vancouver, and Yellowknife (Figure 12a). Also, the values of  $M_{MAX}$  for  $\xi = 50\%$  are 56% and 52%, 90% 79% and 43% of the values of  $M_{MAX}$  for  $\xi = 100\%$  for Ottawa, Edmonton St. John's, Vancouver, and Yellowknife, respectively (Figure 12b).

The air leakage in buildings has consistently improved since the 1990s when the NBCC began to mandate a 'designated' air barrier system. The air barrier system is to provide a 'designated' element to be the 'principal plane of airtightness' and accessories and components to maintain continuity of the airtightness across joints and penetrations. The value of the air leakage rate for an air barrier system was recommended as  $0.1 \text{ L}/(\text{s}\cdot\text{m}^2)$  at a pressure difference of 75 Pa, for typical indoor winter conditions of 27% to 55% RH at 21°C. This recommended air leakage rate was introduced in the 1995 NBCC [19] and continues to be referenced in the 2010 NBCC (A-5.4.1.2. (1) & (2)) [7].

### Effect of Inboard and Outboard Insulation

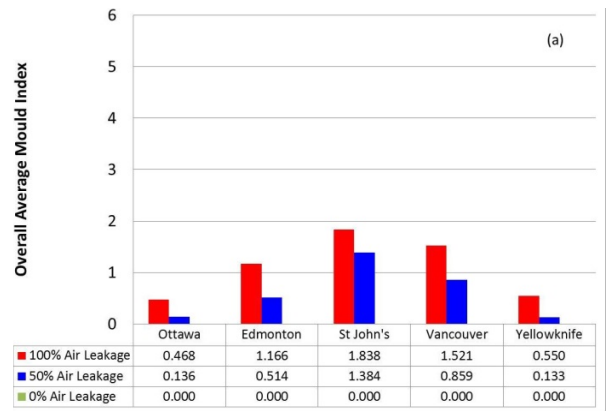
In a previous NRC project [4] and for the case of a 100% air leakage rate, numerical simulations were conducted to investigate the effect of the inboard (stud-cavity) insulation on the risk of condensation and mold growth for different wall assemblies. In that project [4], two types of stud-cavity fibre insulation products having nominal R-values of RSI-3.35 (R-19) and RSI-4.23 (R-24) were investigated for wall systems with and without outboard insulation, and having a wide range of R-values (R-4, R-5 and R-6) and values of WVP (2 to 1800 ng/(Pa·s·m<sup>2</sup>)), when these walls were subjected to the climates of Ottawa, Edmonton, St. John's and Vancouver. The results of that study [4] showed that the wall systems having stud-cavity insulation of R-24 have a higher risk of condensation and mold growth than that for wall systems with stud-cavity insulation of R-19. The other NTRC project [2] focuses on wall systems with stud-cavity insulation of R-24. In this paper, however, as an example, simulations were conducted when the EPS wall, XPS wall and mineral fibre wall have stud-cavity insulation of R-19 and R-24 when these walls were subjected to the climate of Edmonton.

Figure 13a and Figure 13b, respectively, show the overall average mold index ( $M_{AVG}$ ) and overall maximum mold index ( $M_{MAX}$ ) in different wall assemblies. For the purposes of comparison, the performance of the code-compliant reference wall that was obtained in a previous NRC project [4] is included in these figures. As shown in these figures, increasing the R-value of the stud-cavity insulation resulted in a slightly higher risk of condensation and mold growth. For example, the values of  $M_{AVG}$  for walls having R-24 stud-cavity insulation were 5% (reference wall), 4% (EPS wall), 14% (XPS wall) and 15% (mineral fibre wall) higher than that for a wall having R-19 stud-cavity insulation (Figure 13a). The corresponding values of  $M_{MAX}$  for walls having R-24 stud-cavity insulation were 5%, 4%, 14% and 15% higher than that for walls having R-19 stud-cavity insulation (Figure 13b).

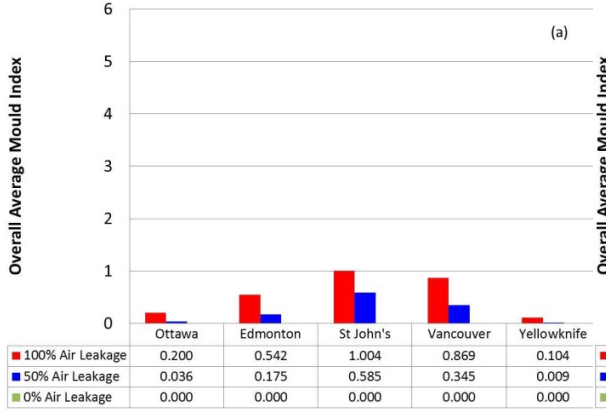
The higher the R-value of the outboard, exterior insulation (R-0, R-3.9, R-10.0 and R-12.5 for Reference wall, EPS wall, XPS wall and mineral fibre wall, respectively), the warmer the wall cavity temperature, and consequently, the less likely the formation of interstitial condensation occurring during the cold periods, and hence the lower the mold index. As shown in Figure 13a, the values of  $M_{AVG}$  for the EPS wall, XPS wall and mineral fibre wall, respectively, were 59%, 27% and 23% of the value of  $M_{AVG}$  for the reference wall. Also, the corresponding  $M_{MAX}$  values for these walls were 68%, 31% and 26% of that for the reference wall (Figure 13).

Comparisons for the yearly heat losses in winter season and yearly heat gains in the summer season for the reference wall and walls with exterior insulations with stud-cavity insulations of R-19 and R-24 are provided in Figure 14 and Figure 15, respectively, for both the average year and wet year. It is important to point-out that the yearly heat losses and yearly heat gains shown in these figures are the heat losses in the wall systems and are not necessarily the heat losses one can expect in a house. Note that the summer season in this paper was defined as when the outdoor temperature was greater than the indoor temperature, and vice versa for the winter season.

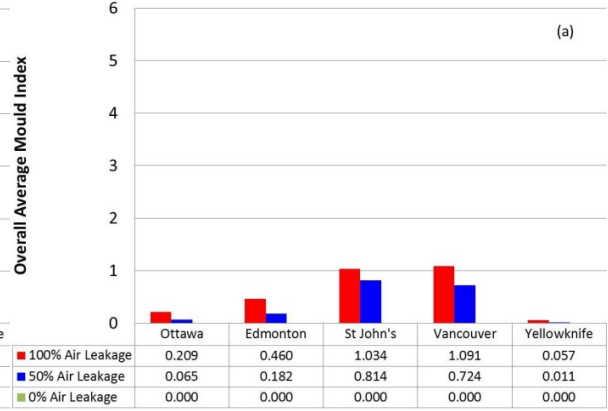
As shown in Figure 14 and Figure 15, increasing the stud-cavity thermal resistance resulted in a decrease in both yearly heat loss and yearly heat gain. For example, the yearly heat losses of walls with R-24 stud-cavity were 22%



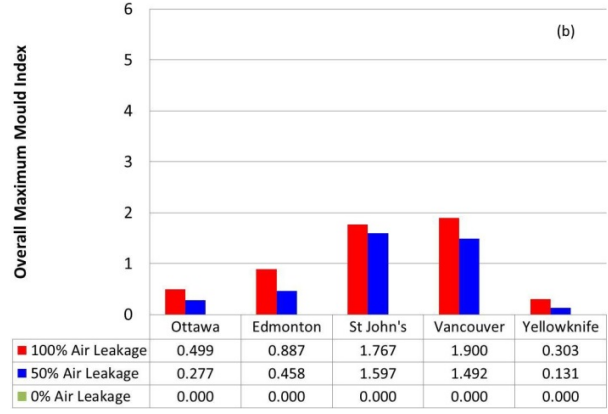
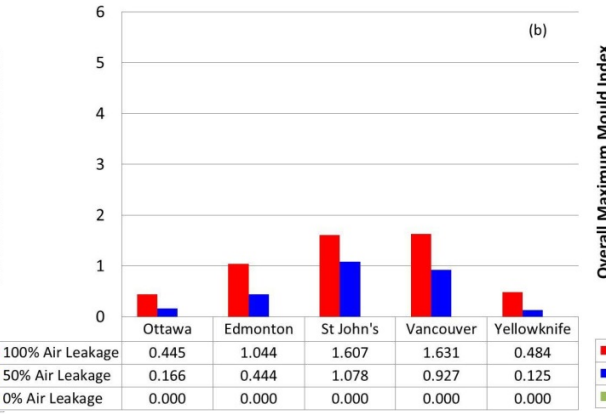
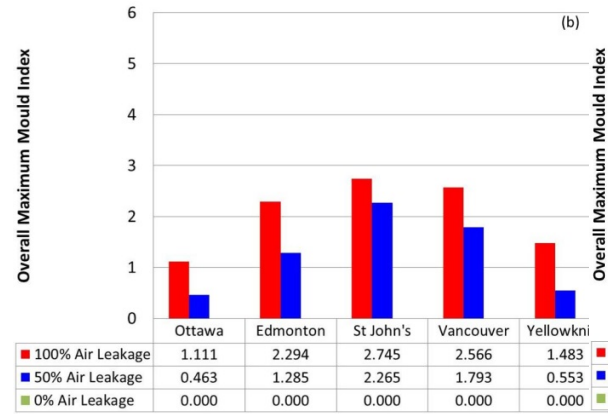
**Figure 10.** Wall 1 (EPS) - Effect of air leakage rate on overall (a) average & (b) maximum mould index



**Figure 11.** Wall 2 (XPS) - Effect of air leakage rate on overall (a) average & (b) maximum mould index



**Figure 12.** Wall 3 (Mineral fibre) - Effect of air leakage rate on overall (a) average & (b) maximum mould index



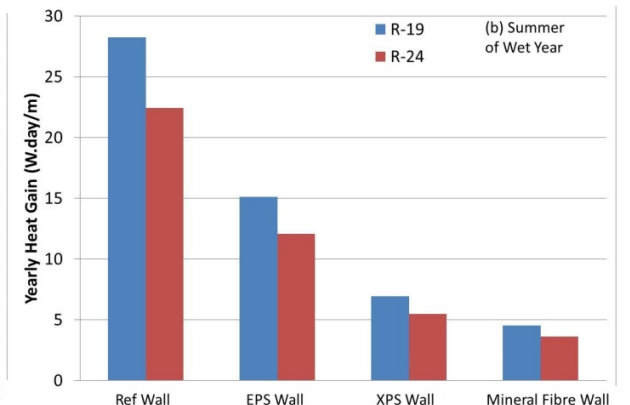
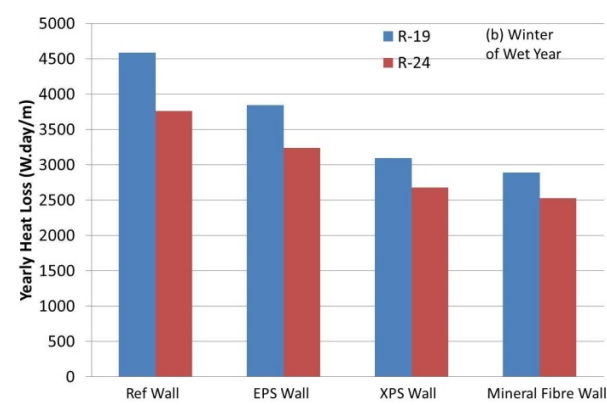
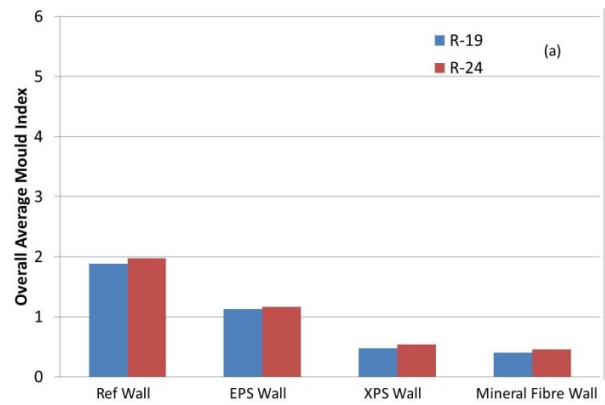
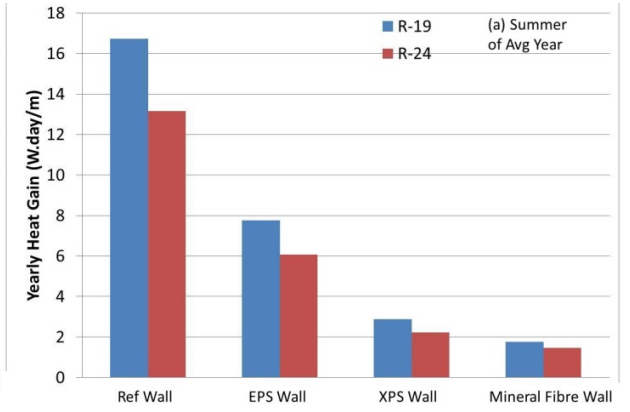
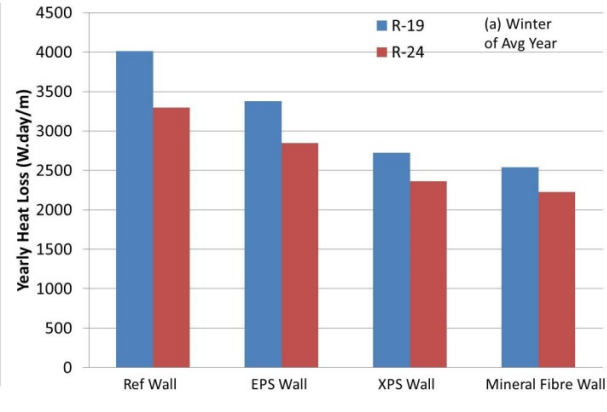
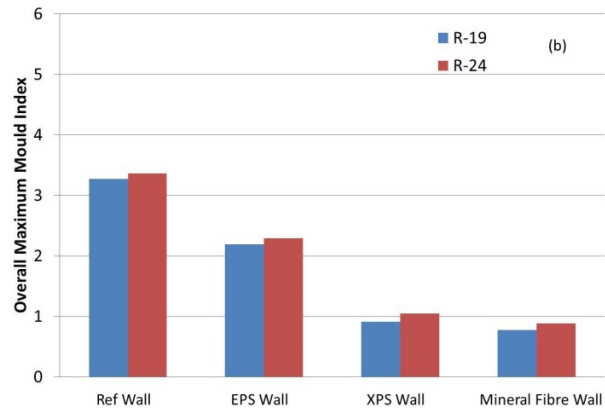


**Figure 13.** Effect of stud-cavity insulation on the overall maximum and average mould index at 100% air leakage rate (Edmonton weather)

**Figure 14.** Effect of stud-cavity insulation on the yearly heat loss at 100% air leakage rate (Edmonton weather)

**Figure 15.** Effect of stud-cavity insulation on the yearly heat gain at 100% air leakage rate (Edmonton weather)

(reference wall), 19% (EPS wall), 15% (XPS wall) and 14% (mineral fibre wall) lower than that for walls with R-19 stud-cavity. Conversely, as indicated above, the risk of condensation and mold growth for walls with R-24 stud-cavity was 4% – 15% higher than the walls with R-19 stud-cavity. Note that the percentage decrease in the heat loss for wall with R-24 as compared to wall with R-19 was for the case of 100% air leakage rate. Considering a lower air leakage rate, however, would result in greater percentage decrease in the heat loss for wall with R-24 as compared to wall with R-19.

Adding outboard, exterior insulation not only decreases the yearly heat losses and yearly heat gains (see Figure 14 and Figure 15), but also decreases the risk of condensation and mold growth as explained earlier (see Figure 13). For example, the yearly heat losses of walls with R-19 stud-cavity were 19% (EPS wall with R-3.9), 47% (XPS wall with R-10.0) and 58% (mineral fibre wall with R-12.5) lower than that for the reference wall (no exterior insulation). The corresponding yearly heat losses of walls with R-24 stud-cavity were 16%, 39% and 48%, respectively, lower than that for the reference wall.

For the case of stud-cavity insulation of R-24, similar comparisons for the yearly heat loss and yearly heat gain for the reference wall and wall systems with exterior insulations are provided in reference [2].

In summary, the yearly heat loss and heat gain are lower for walls with R-24 stud-cavity insulation than that for walls with R-19 stud-cavity insulation, but the risk of condensation in the former is higher than that in latter. For a given stud-cavity insulation, wall systems having additional exterior insulation resulted not only in higher energy performance but also lower risk of condensation and mold growth than walls without exterior insulation.

### Effect of Geographical Locations

The hygrothermal performance for different wall assemblies (see Table 2) were obtained when these walls were subjected to the climates of five Canadian cities each differing in geographical location and that included: Ottawa (ON), Edmonton (AB), Vancouver (BC), St. John's (NL) and Yellowknife (NT). The primary environmental parameters that greatly affected the hygrothermal performance related to the risk of condensation and mold growth were the:

- Outdoor temperature which can be represented by the Heating Degree Days (HDD). The greater the number of HDD the higher the risk for mold growth in a wall assembly. Amongst the geographical locations considered in this study, Yellowknife had the highest HDD (HDD = 8170), followed by Edmonton (HDD = 5120).
- Outdoor relative humidity which can be represented by the Moisture Index (MI). The higher the MI value, the smaller the drying potential of a wall assembly and hence, the higher the risk of mold growth. Amongst the geographical locations considered in this study, Vancouver had the highest value of MI (MI = 1.44), followed by St. John's (MI = 1.41).
- Wind speed; the higher the wind speed, the greater the air leakage rate across the wall assembly, and hence, the higher the risk for mold growth within the wall assembly as indicated earlier.

Details for determining the air leakage rates of the different geographical locations are provided in reference [4]. Also, the air leakage rates of the different locations are provided in [2, 4]. Amongst the geographical locations considered in this study, St. John's provided the highest air leakage rate across wall assemblies (see [2, 4]).

**Figure 16a** and **Figure 16b** show a comparison of the overall average value for mold index ( $M_{AVG}$ ) and overall maximum value of mold index ( $M_{MAX}$ ) for different wall assemblies having R-24 as stud-cavity insulation at a 100% air leakage rate when subjected to different climatic conditions. As shown in these figures, the combined effects of the three environmental parameters, listed above, have brought about, in the case of walls subjected to the climatic conditions of Ottawa and Yellowknife, the lowest value of mold index.

For example, the overall average values for mold index for the reference wall were 1.18, 1.98, 2.41, 3.05 and 1.06, respectively, for the climatic conditions of Ottawa, Edmonton, Vancouver, St. John's and Yellowknife (**Figure 16a**). Whereas the highest value of overall average mold index can be found for the reference wall, EPS wall and XPS wall subjected to the climatic conditions of St. John's. For the mineral fibre wall subjected to the climatic conditions of St. John's and Vancouver, the values of overall average mold (1.03 and 1.09,

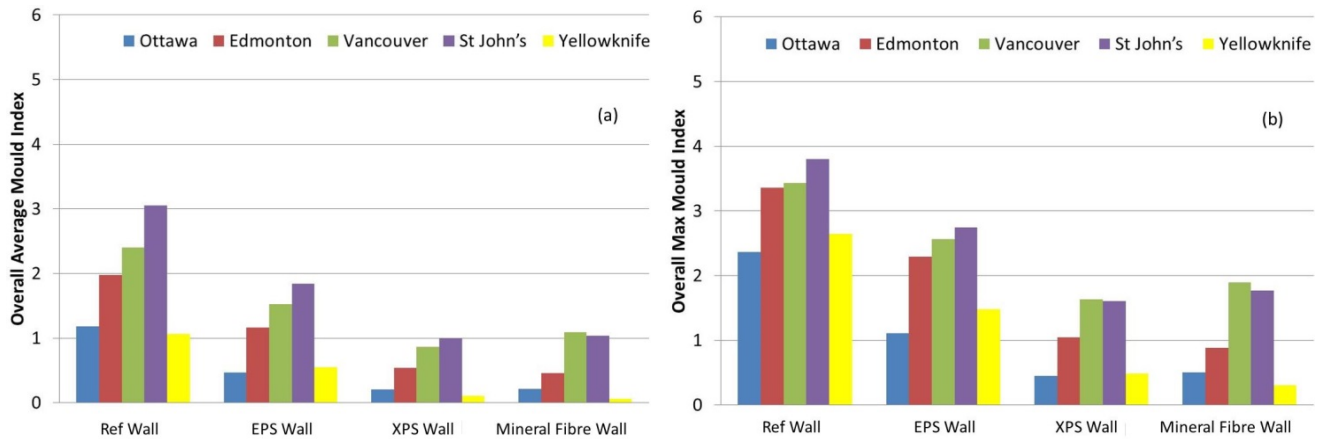


**Figure 16.** Effect of geographical locations on overall maximum & average mold index at 100% air leakage rate

respectively) were approximately the same. Details about the risk of condensation and mold growth in wall assemblies with exterior insulation over a broad range of values for thermal resistance (e.g. R-values of 4, 5 and 6 ft<sup>2</sup>•h•oF/BTU) and WVP (2 to 1800 ng/(Pa•s•m<sup>2</sup>)) and subjected to different climatic conditions are available in reference [2].

## SUMMARY OF SIMULATION RESULTS FOR DIFFERENT WALLS

For all wall assemblies having R-24 stud-cavity insulation and with 100% air leakage rate, the results of the risk of mold growth are presented in the following order: Edmonton, Ottawa, Vancouver, Yellowknife and St. John's, where:

- Figure 17 for Edmonton, AB (cold, dry climate with HDD18 = 5120, MI = 0.48),
- Figure 18 for Ottawa, ON (cold, dry climate with HDD18 = 4440 to 4500, MI = 0.84),
- Figure 19 for Vancouver, BC (mild, wet climate with HDD18=2600 to 3100, MI = 1.44);
- Figure 20 for Yellowknife, NT (cold, dry climate with HDD18 = 8170, MI = 0.58); and
- Figure 21 for St. John's, NL (mild, wet climate with HDD18 = 4800, MI = 1.41).

The results of thermal performance of these wall systems expressed in terms of the yearly heat losses and gains, are available in [4].

### Edmonton, AB

As might be expected, increasing the R-value of the outboard, exterior insulation (Table 2) decreases the overall average value of  $M_{AVG}$  and overall maximum value,  $M_{MAX}$ . In Figure 17 is shown that in all instances, the values derived for both  $M_{AVG}$  and  $M_{MAX}$  for wall assemblies with exterior insulation are less than those for the code-compliant reference wall (Figure 17a). The values for  $M_{AVG}$  for these walls range from 1.98 to 0.46; corresponding values for  $M_{MAX}$  of these walls range from 0.89 to 3.36 (Figure 17b).

### Ottawa, ON

As was the case for Edmonton, in all instances, the values derived for the overall average mold index and overall maximum mold index for walls with exterior insulations are less than those for the reference wall. The values derived for  $M_{AVG}$  for all wall assemblies range from 1.18 to 0.20 (Figure 18a). The corresponding values for  $M_{MAX}$  for these walls range from 2.37 to 0.44 (Figure 18b). As compared to the results obtained for Edmonton, however, the values for  $M_{AVG}$  and  $M_{MAX}$  for these sets of walls are lower. For example, the values of  $M_{AVG}$  of reference wall and EPS wall are 1.18 and 0.47, respectively, for Ottawa (Figure 18a), whereas for Edmonton these values are 1.98 and 1.17 (Figure 17a). The corresponding values of  $M_{MAX}$  are 2.37 and 1.11 for Ottawa (Figure 18b), whereas for Edmonton (Figure 17b) these values are 3.36 and 2.29.

## Vancouver, BC

Values of  $M_{AVG}$  and  $M_{MAX}$  for walls subjected to a Vancouver climate are comparatively greater than that of Ottawa, and slightly greater than those of Edmonton. As shown in Figure 19a, the values for  $M_{AVG}$  for these walls range from 2.41 to 0.87. The corresponding values for  $M_{MAX}$  for these walls range from 3.43 to 1.63 (Figure 19b).

## Yellowknife, NT

Values of  $M_{AVG}$  and  $M_{MAX}$  for walls subjected to a Yellowknife climate are approximately the same as that of Ottawa. As shown in Figure 20a for Yellowknife, the values for  $M_{AVG}$  for different wall systems range from 1.06 to 0.06 compared to the range of 1.18 to 0.21 for Ottawa (Figure 18a). The corresponding values for  $M_{MAX}$  for these walls range from 2.65 to 0.30 for Yellowknife (Figure 20b) and from 2.37 to 0.44 for Ottawa (Figure 18b).

## St. John's, NL

The greatest values for the overall  $M_{AVG}$  of the reference, EPS and XPS wall configurations occur in St. John's as compared to the other cities investigated. Note that the St. John's climate has the highest air leakage rate compared to the other geographical locations investigated (see [2, 4] for more details). Also St. John's climate is a wet climate with moisture index ( $MI = 1.41$ ) slightly lower than that of Vancouver climate ( $MI = 1.44$ ). Figure 21a shows that the values for  $M_{AVG}$  for all walls range from 3.05 to 1.0, whereas the corresponding values for  $M_{MAX}$  for these walls range from 3.8 to 1.61 (Figure 21b).

## CONCLUDING REMARKS

NRC's hygrothermal numerical model, hygIRC-C, was first benchmarked against experimental work carried out in the FWEF; the benchmarking exercise consisted of completing transient numerical simulations, as was done in a number of other studies, to benchmark the model against experimental work. The numerical results derived for values of heat flux attained at different locations within the respective wall assemblies were compared with the measured values for assemblies incorporating different exterior insulation products that included: (i) EPS of 1" thick (R-3.9 and WVP = 114), (ii) XPS of 2" thick (R-10 and WVP = 27), and (iii) Mineral fibre insulation products of 3" thick (R-12.5 and WVP = 2130). The results showed that the comparison between the present model predictions and experimental data were in good agreement.

Following the benchmarking of the present model, it was then used to conduct a parametric study to investigate the risk of condensation and mold growth in different wall assemblies when these assemblies were subjected to climatic conditions in Canada, specifically, that of: Vancouver (BC), Edmonton (AB), Ottawa (ON), St. John's (NL), and Yellowknife (NT). The modelling results for the different walls were expressed using values of  $M$  based on the most recent mold growth model developed by Ojanen et al. [18] and from which were obtained values of  $M$  of different materials within the respective wall assemblies.

Based on the air leakage path that was considered in this study, the simulation results showed that the critical locations inside the wall assembly at risk of mold growth are the top and bottom portions of the wall assembly. However, had a different air leakage path been considered in this study, it would have resulted in different locations within the wall assemblies being at risk of condensation and mold growth.

Similar to a previous NRC study [4], the simulation results were presented on the basis of a simple form using the following two parameters; the overall:

- Average value of mold index ( $M_{AVG}$ ): average value of  $M$  at all locations within the assembly;
- Maximum value of mold index ( $M_{MAX}$ ): average value of maximum value of  $M$  at all locations within wall.

A sensitivity analysis was conducted to investigate the effect of different air leakage rates of 0% (no air leakage), 50%, and 100% on the hygrothermal performance of wall assemblies. No risk of condensation occurred in the wall assemblies for the case of no air leakage. The case of 100% air leakage rate (i.e.  $0.1 \text{ L}/(\text{s}\cdot\text{m}^2)$  at 75 Pa) resulted in higher risk of condensation and mold growth than that for the case of 50% air leakage rate (i.e.  $0.05 \text{ L}/(\text{s}\cdot\text{m}^2)$  at 75 Pa).

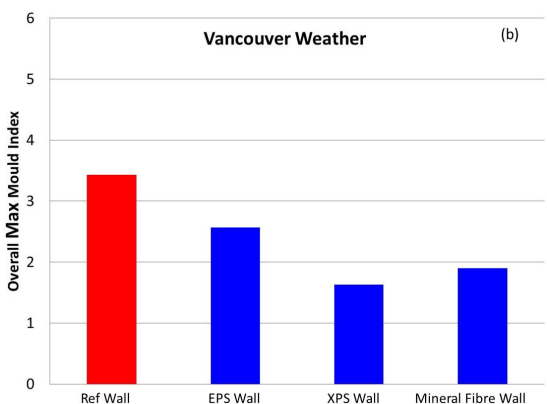
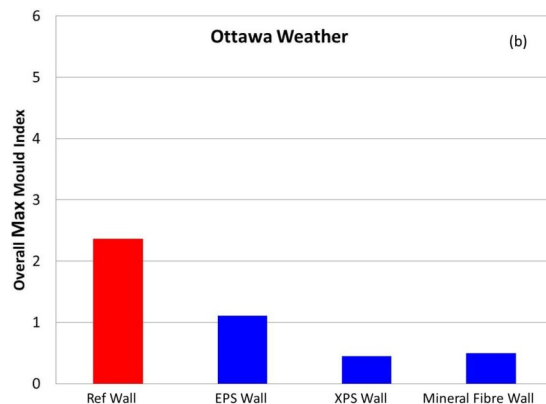
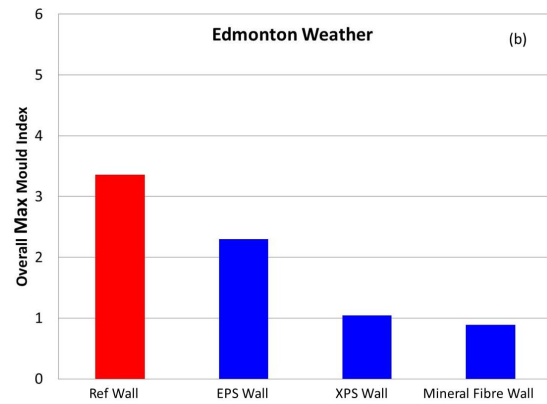
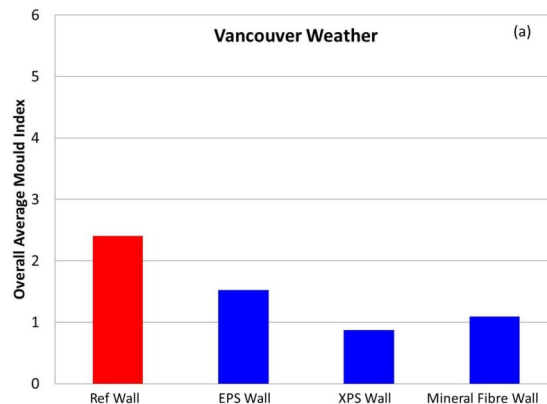
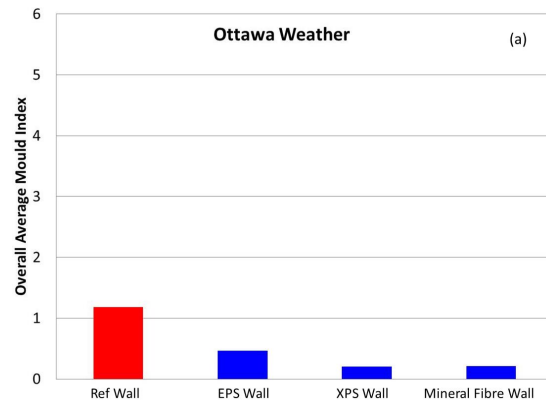
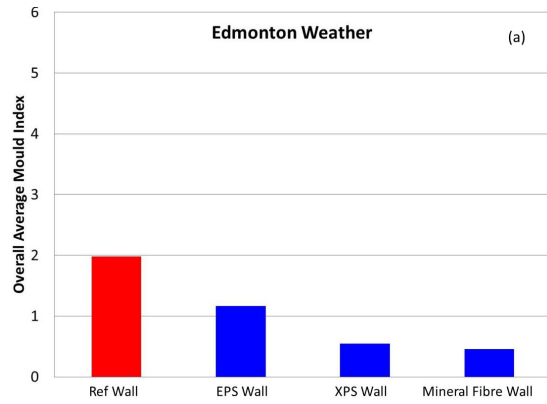


**Figure 17.** Effect of R-value and WVP on overall maximum and average mould index at 100% air leakage rate (Edmonton weather)

**Figure 18.** Effect of R-value and WVP on overall maximum and average mould index at 100% air leakage rate (Ottawa weather)

**Figure 19.** Effect of R-value and WVP on overall maximum and average mould index at 100% air leakage rate (Vancouver weather)

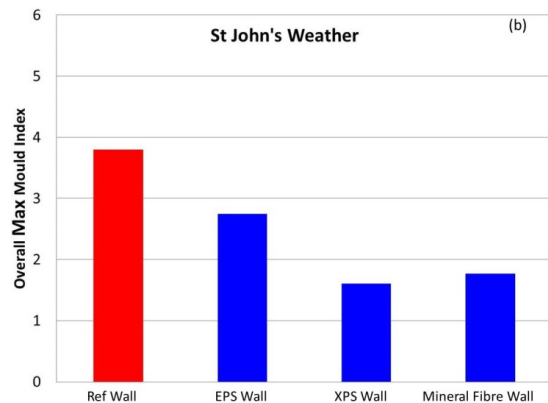
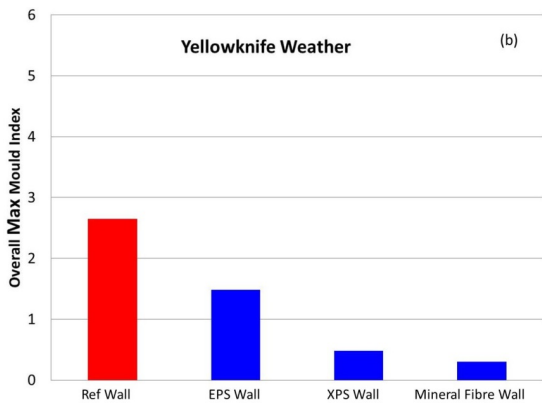
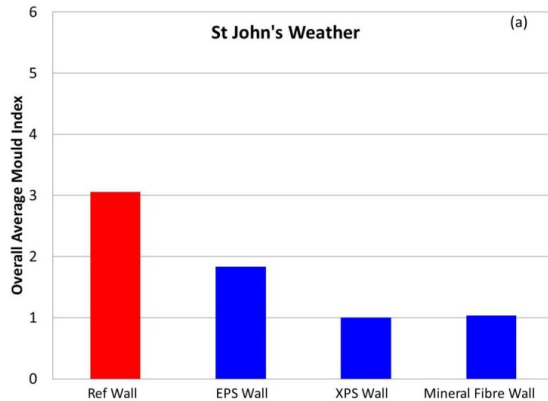
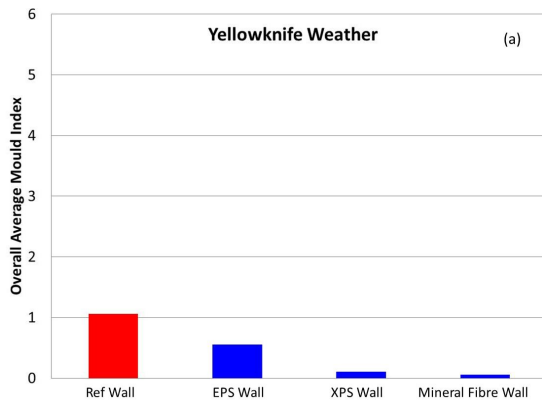


**Figure 20.** Effect of R-value and WVP on overall maximum and average mold index at 100% air leakage rate (Yellowknife weather)

**Figure 21.** Effect of R-value and WVP on overall maximum and average mold index at 100% air leakage rate (St. John's weather)

The values for the overall average mold index and overall maximum mold index in different wall assemblies with the inboard stud-cavity insulation of R-24 were higher than that of walls having stud-cavity insulation of R-19. The values for the overall average mold index and overall maximum mold index in walls with different types of outboard, exterior insulations were lower than that of the code-compliant reference wall.

For the code-compliant reference wall, the EPS wall and XPS wall, St. John's (NL) appeared to have the most severe climate in comparison to the other four locations investigated (Vancouver (BC), Ottawa (ON), Edmonton (AB) and Yellowknife (NT)); the greatest values of the overall average mold index in the wall configurations amongst the five locations occurred in this location. For the wall having mineral fibre as exterior insulation, the values of the overall average mold index were approximately the same for St. John's and Vancouver.

## ACKNOWLEDGMENTS

The authors wish to thank Canada Mortgage and Housing Corporation and Natural Resources Canada for contributing funding for this project. The authors also wish to thank the Project Advisory Committee, including: Constance Thivierge (formerly of FP Innovations), Doug Tarry (Doug Tarry Homes), Rick Gratton and Christopher McLellan (CHBA), Chris Mattock (Habitat Design & Consulting), Salvatore Ciarlo (Owens Corning Canada) and Robert Jonkman (Canadian Wood Council). Thank as well to NRC-Construction for providing funds to enable researchers to build, operate and maintain the Field Exposure of Walls Facility (FEWF) that was used in this project.

## REFERENCES

1. Lacasse, M. A., Saber, H.H., Ganapathy, G., and Nicholls, M., "Evaluation of Thermal and Moisture Response of Highly Insulated Wood-Frame Wall Assemblies — Phase 1; Part I: Experimental trials in Field Exposure of Walls test Facility"; Report No. A1-000444.5; NRC-Construction, National Research Council of Canada, Ottawa, Canada; 12 January, 2016.
2. Saber, H.H., and Ganapathy, G., "Evaluation of Thermal and Moisture Response of Highly Insulated Wood-Frame Wall Assemblies — Phase 1; Part II: Numerical Modelling"; Report No. A1-000444.4; NRC-Construction, National Research Council of Canada, Ottawa, Canada; 8 January, 2016.
3. ASTM Designation: C 1130-07, "Standard Practice for Calibrating Thin Heat Flux Transducers", Annual Book of ASTM Standards, sec 4, Construction, vol. 04.06, Thermal Insulation; Building & Environment Acoustic, pp. 577-584, 2009.
4. Saber, H.H., Maref, W. and Abdulghani, K., Properties and Position of Materials in the Building Envelope for Housing and Small Buildings, Report No. A1-004615.1, NRC-Construction, National Research Council of Canada, Ottawa, Canada, Dec., 31, 2014.
5. Mukhopadhyaya, P., Kumaran, M.K., Lackey, J., Normandin, N., van Reenen, D., Tariku, F. "Hygrothermal properties of exterior claddings, sheathing boards, membranes and insulation materials for building envelope", Proceedings of thermal performance of the exterior envelopes of whole buildings X; pp. 1-16, Clearwater, Florida, USA, December 2-7, 2007.
6. ASHRAE. 2009. 2009 ASHRAE Handbook –Fundamentals (SI), Chapter 26, Atlanta: American Society of Heating, Refrigerating, and Air-Conditioning Engineers Inc.
7. National Building Code of Canada (2010), .Section 9.25, Canadian Commission on Building and Fire Codes National Research Council of Canada, Ottawa, Canada.
8. Ojanen, T. and Kumaran, M.K., "Effect of exfiltration on the hygrothermal behaviour of a residential wall assembly: results from calculations and computer simulations", International Symposium On Moisture Problems In Building Walls, Porto - Portugal, 11 - 13 September, pp. 157, 1995.
9. Saber, H.H., and Maref, W., "Risk of Condensation and Mold Growth in Wood-Frame Wall Systems with Different Exterior Insulations", BEST Building Enclosure Science & Technology Conference (BEST4), held in April 12-15, 2015, Kansas City, Missouri, USA, 19 p.
10. Elmahdy, A.H., Maref, M., Saber, H.H., Swinton, M.C., and Glazer, R., "Assessment of the Energy Rating of Insulated Wall Assemblies a Step Towards Building Energy Labelling", 10th Int. Conference for Enhanced Building Operations (ICEBO2010), Kuwait, Oct. 2010.
11. Elmahdy, A.H., Maref, W., Swinton, M.C., Saber, H.H., and Glazer, R., "Development of energy ratings for insulated wall assemblies", Building Envelope Symposium, San Diego, California, October 26, pp. 21-30, 2009.
12. Saber, H.H., Maref, W., Elmahdy, A.H., Swinton, M.C., and Glazer, R., "3D Thermal Model for Predicting the Thermal Resistances of Spray Polyurethane Foam Wall Assemblies", Building XI conference, Clearwater, Florida, 2010.
13. Saber, H.H., Maref, W., Elmahdy, A.H., Swinton, M.C., and Glazer, R., "3D Heat and Air Transport Model for Predicting the Thermal Resistances of Insulated Wall Assemblies", International Journal of Building Performance Simulation, vol. 5, No. 2, p. 75–91, 2012.
14. ASHRAE 160-2009 Standard - Criteria for Moisture-Control Design Analysis in Buildings (ANSI/ASHRAE Approved), ASHRAE 2009, Atlanta, GA, 16 p.).
15. Glass, S.V., Hygrothermal Analysis of Wood-Frame Wall Assemblies in a Mixed-Humid Climate, United States Department of Agriculture, Forest Service, Forest Products Laboratory, Research Paper FPL–RP–675, pp. 1-25, April 2013.
16. Hukka, A., and Viitanen, H.A., "A mathematical model of mold growth on wooden material, Wood Science and Technology", vol. 33 (6), pp 475-485, 1999.
17. Viitanen, H.A., and Ojanen, T., "Improved model to predict mold growth in building materials" Proceedings of Thermal Performance of the Exterior Envelopes of Whole Buildings X, 8 p., 2007.
18. Ojanen, T., Viitanen, H.A., Peuhkuri, R., Lähdesmäki, K., Vinha, J., and Salminen, K., "Mold Growth Modeling of Building Structures Using Sensitivity Classes of Materials", 11th International Conference on Thermal Performance of the Exterior Envelopes of Whole Buildings XI (Clearwater, (FL), USA, December-05-10), 10 p., 2010.
19. National Building Code of Canada (1995), Canadian Commission on Building and Fire Codes, National Research Council of Canada, Ottawa, Canada.

Hamed H. Saber, Michael A. Lacasse, G. Ganapathy, Silvio Plescia, Anil Parekh